

THE TEMPERATURE OF THE COSMIC MICROWAVE BACKGROUND

D. J. FIXSEN

University of Maryland, Goddard Space Flight Center, MD, USA

Received 2009 October 6; accepted 2009 October 28; published 2009 November 30

ABSTRACT

The Far InfraRed Absolute Spectrophotometer data are independently recalibrated using the *Wilkinson Microwave Anisotropy Probe* data to obtain a cosmic microwave background (CMB) temperature of 2.7260 ± 0.0013 . Measurements of the temperature of the CMB are reviewed. The determination from the measurements from the literature is CMB temperature of 2.72548 ± 0.00057 K.

Key words: cosmic microwave background – cosmology: observations

1. INTRODUCTION

The *Wilkinson Microwave Anisotropy Probe* (*WMAP*) data present an opportunity to recalibrate the Far-InfraRed Absolute Spectrophotometer (FIRAS) experiment and produce an independent check of the other measurements of the cosmic microwave background (CMB) temperature. In Sections 2 and 3, the *WMAP* data will be presented and combined with the FIRAS data to make an independent estimate of the CMB temperature. In Sections 4 and 5, this new estimate will be combined with others from the literature to generate an improved estimate for the CMB temperature.

The *WMAP* data only measure the difference in intensity between different points on the sky. However, the precision is sufficient such that the velocity of the *WMAP* spacecraft can be used to calibrate the velocity to various points on the surface of last scattering of the CMB. This velocity in turn is used to form a differential spectrum of the CMB. The differential spectrum is then fit with a single parameter which is the CMB temperature.

2. *WMAP* VELOCITY MAP

The standard *WMAP* sky maps (Hinshaw et al. 2009) are corrected to the barycenter of the solar system using the JPL ephemeris (Standish & Fienga 2002). The calibration assumes a CMB temperature of 2.725 K (derived from the FIRAS measurement). However, the various changes as the *WMAP* makes its way around the Sun (now in its ninth repetition) can be used to calibrate the *WMAP* data in terms of velocity. The velocity of the *WMAP* spacecraft, with respect to the Sun, is known to $< 1 \text{ cm s}^{-1}$, which is a negligible uncertainty compared to other uncertainties considered here. This velocity is used to calibrate a map of velocity relative to the surface of last scattering of the CMB. Most of this velocity is the dipole, presumably the motion of the solar system with respect to the frame of the CMB; however, it includes temperature variations due to the Sachs–Wolfe effect which has the same spectrum. This process is repeated for each *WMAP* differential assembly and each year yielding 50 independent maps for the first five years of *WMAP* operation.

The *WMAP* velocity maps are the temperature maps, available at http://lambda.gsfc.nasa.gov/product/map/current/m_products.cfm, with the dipole added back in and divided by the CMB temperature. In generating the *WMAP* temperature maps, a dipole is fit and removed from the raw data. The residual variations are due to various sensitivities of the *WMAP* instrument—the changing velocity as the spacecraft makes its

annual trek around the solar system and the small variations of the CMB as a function of position. The *WMAP* team has done an excellent job of removing the instrumental effects. By correcting the velocity to the barycenter of the solar system, the effects of the spacecraft velocity are also removed. But this information also allows the calibration of the *WMAP* data. But the information is in velocity rather than temperature. In order to get the temperature for the published maps an absolute temperature must be assumed. The *WMAP* team used 2.725 K from the previous FIRAS measurements to translate the velocity measurements into temperature units. To get the velocity maps, the data are divided by 2.725 K to restore the velocity calibration in units of v/c . The dipole ($v/c = 0.0012338$, $l = 263^\circ 87$, $b = 48^\circ 24$) is added back in to restore the full velocity. The fitting includes an absolute term which is treated as a nuisance parameter so no absolute adjustment to the *WMAP* data is required or made.

No corrections to the *WMAP* data are made for Galactic foregrounds. The maps are convolved with the FIRAS beam (approximately a 7° top hat) to produce maps with the FIRAS resolution. These maps are produced with the pixelization of the native FIRAS data.

For each velocity map, the FIRAS data (also available on the lambda website) are fit to a set of 10 templates, shown in Figure 1. The first template is unity everywhere. This template is included to model the monopole. The second template is one of the velocity maps from the *WMAP* data. The remaining eight maps are included to fit various foregrounds. These templates include the FIRAS C II and N II maps (Fixsen et al. 1999). The band 8 and 10 DIRBE data also from the COBE mission and a model of the zodiacal emission from the DIRBE team (Kelsall et al. 1998). Also included are an H I map (Dickey & Lockman 1990; Hartmann & Burton 1997), an Aluminum-26 emission line map (Diehl et al. 1995) and the Haslam 408 MHz map (Haslam et al. 1981). The maps not derived from FIRAS data are convolved with the FIRAS beam. Templates 3–10 are included to attempt to fit all local features even though many subsets of them would do almost as well. Since there are 6063 pixels the eight templates make an insignificant reduction in the total number of degrees of freedom.

The FIRAS data are arbitrarily cut off at 1 THz since the CMB spectrum is essentially zero beyond that frequency, and the uncertainty of the FIRAS data at high frequencies is not important for this analysis. The fits use the weight map of the FIRAS low-frequency data (which is nearly identical in form to the high-frequency weight map). Each frequency is fit separately and so each template generates a spectrum for each fit. All of the spectra except the spectrum associated with the velocity are

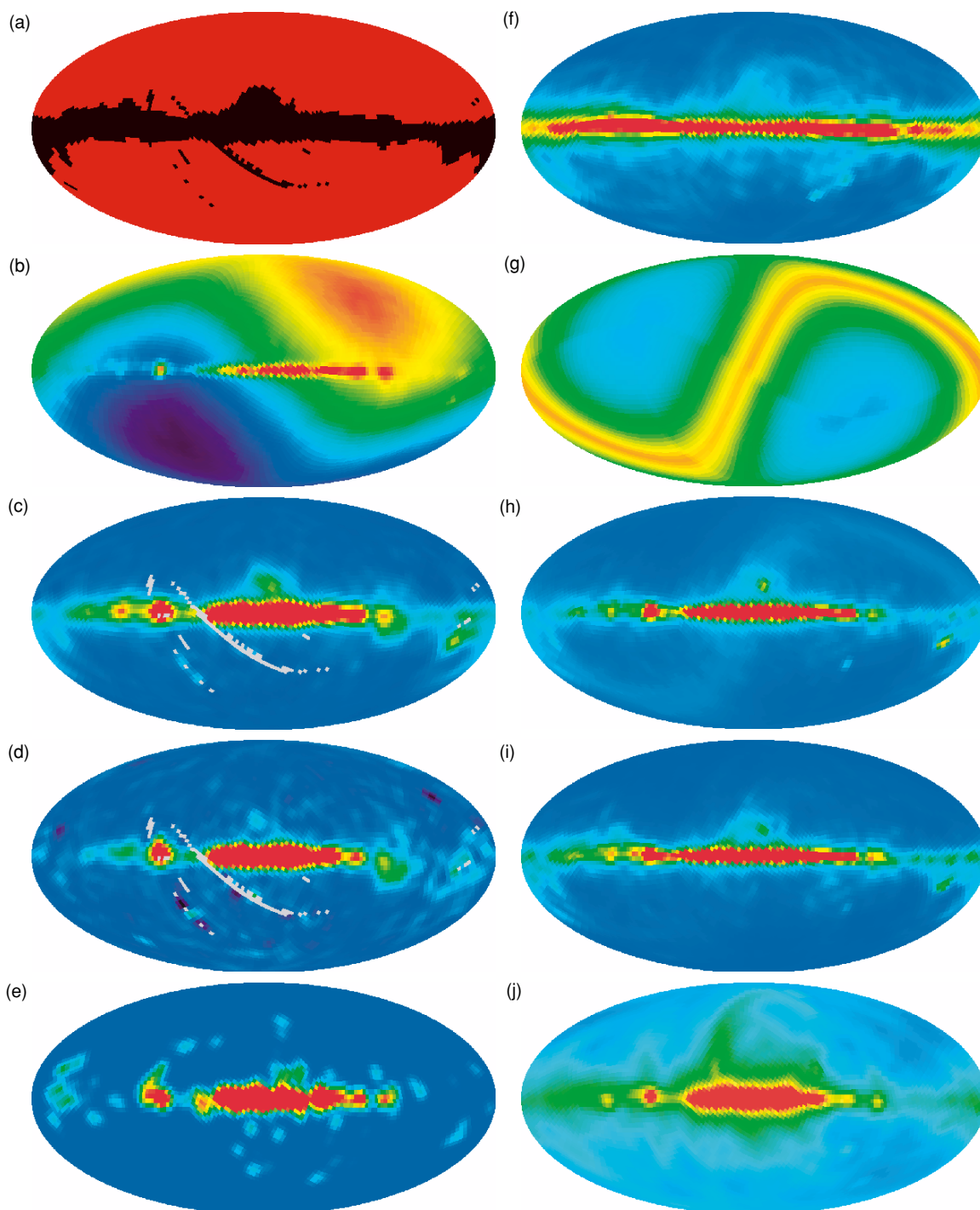


Figure 1. Templates used to fit the FIRAS data. The templates are in Galactic coordinates with the center of the Galaxy in the center of each Mollweide projection. The Galactic equator is a horizontal line across the middle of each figure. From top to bottom the templates are (a) data mask, (b) *WMAP* velocity, (c) C II, (d) N II, (e) A126, (f) H I, (g) Zodiacal model, (h) DIRBE band 8, (i) DIRBE band 10, and (j) Haslam 408 MHz.

treated as nuisance parameters. These increase the uncertainty but are otherwise unused.

Even with these templates the Galactic plane is too large of a perturbation to be insignificant. So the pixels with the largest DIRBE band 10 signal are excluded from the fit. The process was tested with 0%–90% of the data excluded. Figure 2 shows the average estimated temperature for all 50 *WMAP* channels and years as a function of the fraction of excluded data. For less than 5% of the data excluded, significant variations are seen. The variations are concentrated in the 22 GHz (K-band) templates.

If more than 50% of the data are excluded the uncertainties are significantly larger, not only due to the data loss but also due to the loss of the hot and cold ends of the CMB dipole. The results that follow are for 15% of the data excluded. These fits, done independently at each frequency, result in 50 spectra.

3. CMB VELOCITY TEMPERATURE

The average of the 50 spectra is shown in Figure 3. Since this spectrum is associated with the velocity of the solar system

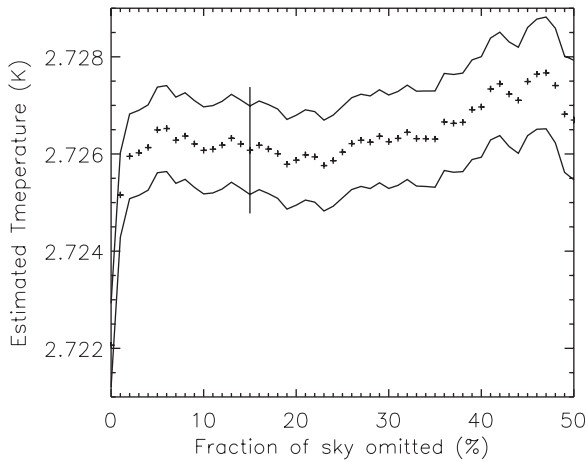


Figure 2. Crosses are the CMB temperature estimation for a given fraction of the brightest part of the sky excluded. The lines are the nominal $+1\sigma$ and -1σ limits. The error bar is the adopted value and uncertainty inflated for the excess χ^2 .

with respect to the CMB (and some Sachs–Wolfe effect), the spectrum appears not as an absolute spectrum but as a differential spectrum generated by the Doppler shift.

According to the special theory of relativity the spectrum observed in a reference frame moving with respect to the source of a blackbody spectrum, $B(T, \nu)$, at temperature T , is shifted such that

$$S'(\nu) = B\left(T\sqrt{\frac{1+v}{1-v}}, \nu\right), \quad (1)$$

where ν is the frequency, and v is the velocity toward the source divided by the speed of light.

Thus ignoring negligible second-order terms and higher, we have

$$S(\nu, p) = B(T, \nu) + v(p)T \frac{\partial B(T, \nu)}{\partial T} \Big|_{T=T_0}, \quad (2)$$

where the spectrum is now a function of position, P , on the sky. Note that the first term is absorbed in the first template. The remaining term $vT\partial B/\partial T$ is the term related to the second template. The velocity, v , is already included in the template; thus, the term to fit is $T\partial B/\partial T$, which must match the spectrum. Although strictly speaking this is nonlinear, a spectrum $T\partial B/\partial T$ for a T near the CMB temperature (say 2.726 K) can be subtracted from the spectrum and, the residual can then be fit to $\delta T(\partial B/\partial T + T\partial^2 B/\partial T^2)$ for the small δT correction. Since both the process of averaging the velocity maps and the spectral fitting are linear processes, they can be done in either order. So the average spectrum is fit with a result of $T = 2.7260$.

3.1. FIRAS Uncertainty

The uncertainty of the temperature is dominated by the noise in the FIRAS measurements. Propagating the uncertainties shown in Figure 3 results in an uncertainty estimate of 0.74 mK, but this does not include the correlations amongst the different frequencies. Including the correlations and the PEP error term, which is important in this context (Fixsen et al. 1994), results in an uncertainty estimate of 1.09 mK. The χ^2 is 98.7 for 69 degrees of freedom (DOF). Since the χ^2 is higher than expected the uncertainty is inflated to produce a χ^2 per DOF of unity with a resulting uncertainty of 1.3 mK in the CMB temperature due to the uncertainties of the FIRAS measurements.

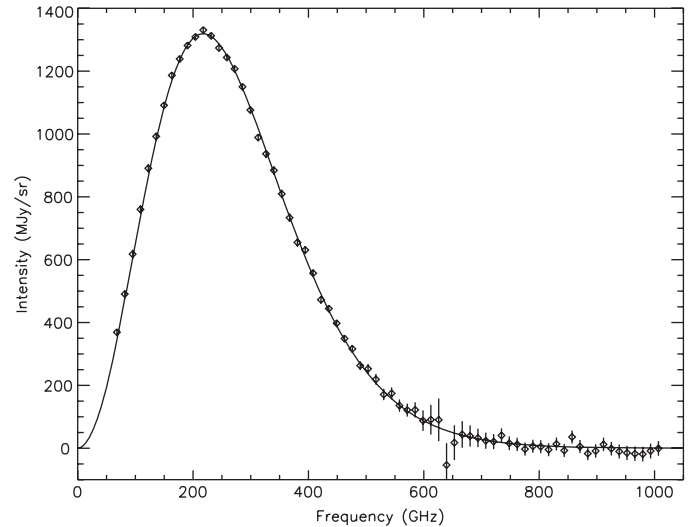


Figure 3. Mean spectrum associated with the velocity of the solar system with respect to the CMB. The line is the a priori prediction based on the *WMAP* velocity and the previous FIRAS calibration. The uncertainties are the noise from the FIRAS measurements. The error bars are slightly misleading, because they do not show the correlations, but the correlated errors are properly treated in the fit.

In deriving the FIRAS dipole (Fixsen et al. 1996) amplitude the only term is the $\delta T\partial B/\partial T$. Here the second term $\delta T T\partial^2 B/\partial T^2$ is both larger and at a mean higher frequency. This allows a more precise determination of the temperature. Also the velocity map allows more control of the systematic effects from the cut. Some of the variations due to the cuts was due to higher order ($l > 1$) variation in the CMB. Here the variation in the CMB is included in the velocity maps, so neither of these terms add to the uncertainty.

3.2. WMAP Uncertainty

The uncertainty from the *WMAP* measurements also needs to be included. The RMS variation in the gains ($\Delta\nu/\nu$) of the 50 independent *WMAP* maps is 0.00096. Nominally, the uncertainty of the mean of such a set would be 0.00014. Figure 7 of Hinshaw et al. (2009) indicates a .001 uncertainty for each of 40 individually calibrated data channels which results in a similar uncertainty estimate for the mean.

But at the level of 0.00014, the *WMAP* uncertainties are insignificant. Even if the uncertainty were 0.0005, the *WMAP* data would not then be a significant source of uncertainty. If the mean error were 0.0016, the *WMAP* uncertainty would equal the uncertainty from the FIRAS uncertainty, and the final uncertainty would be increased by a factor of $\sqrt{2}$. Each *WMAP* channel and year is processed independently. Unless there is a serious unexplained error in the *WMAP* data that correlate both channels and years, the uncertainty of the *WMAP* data is insignificant relative to the uncertainty in the FIRAS data.

The fitted temperatures for each *WMAP* channel and year are shown in Table 1. The average is 2.7260 K with a standard deviation of 0.6 mK. The implied uncertainty of the mean is 0.09 mK. The standard deviation is smaller than expected because a significant part of the variation of the *WMAP* velocity maps is concentrated in the Galactic plane. The 0.09 mK does not include the common uncertainty of the *WMAP* velocity maps or the FIRAS errors.

Combining the uncertainties of the FIRAS and *WMAP* in quadrature results in an uncertainty of 1.3 mK. This

Table 1Estimated CMB Temperatures for the Various Years and *WMAP* Channels

<i>WMAP</i>	Year 1	Year 2	Year 3	Year 4	Year 5
K	2.72511	2.72517	2.72522	2.72512	2.72519
Ka	2.72532	2.72530	2.72526	2.72529	2.72544
Q1	2.72555	2.72541	2.72540	2.72546	2.72557
Q2	2.72553	2.72548	2.72538	2.72543	2.72544
V1	2.72625	2.72627	2.72621	2.72620	2.72639
V2	2.72653	2.72622	2.72630	2.72626	2.72662
W1	2.72624	2.72616	2.72644	2.72635	2.72634
W2	2.72681	2.72682	2.72656	2.72665	2.72650
W3	2.72675	2.72678	2.72649	2.72686	2.72714
W4	2.72712	2.72685	2.72617	2.72580	2.72658

Note. All of these fits are with the brightest 15% of the sky excluded.

measurement is unaffected by absolute systematic errors of either FIRAS or *WMAP* as it uses only differential measurements of both experiments. Further it is insensitive to long-term offset drifts in either instrument as the measurement is dominated by the measurement at the precession period of the *WMAP* data (about 60 minutes) and the orbital period of the COBE spacecraft (about 100 minutes).

In particular, it does not depend on the absolute calibration of the FIRAS thermometers although it does depend on the gain calibration of the FIRAS external calibrator thermometers. It also is relatively insensitive to the FIRAS frequency calibration as the measurement uncertainty is dominated by the amplitude of the spectrum.

The diamonds in Figure 3 are the spectra derived from the FIRAS data. The uncertainties shown are also derived from the FIRAS data. Note the line in Figure 3 is not a fit but the predicted line from the previous $T = 2.725$ FIRAS calibration. The best fit is 2.7260 ± 0.0013 K. The feature at $\nu = 630$ GHz, including the larger uncertainty, is due to the dichroic filter separating the low and high frequencies in the FIRAS instrument.

4. CMB TEMPERATURE

There were many publications of measurements of the CMB temperature from the late '60s and '70s, but the uncertainties are large and the systematics were not well understood. Here an arbitrary cutoff of 50 mK uncertainty was used to select 15 sources for the CMB temperature from recent publications. These results are shown in Table 2.

The weight of the measurements is dominated by the FIRAS measurements, but it is still instructive to look at the other measurements. The measurements using CN are entirely different from any of the other measurements, but the combined CN measurements are 2.742 ± 0.017 K, which is only one sigma high. The rocket measurement from Gush et al. (1990) is like the FIRAS measurement in that it uses a Fourier transform spectrometer, but it has an independent calibrator and independent thermometers. The other measurements depend on external calibrators as the absolute reference, but these are comparatively narrow bands on the low frequency side of peak of the CMB radiation. The χ^2 for the 16 measurements is 17.9 for 15 DOF. A χ^2 this large should be expected about 26% of the time. Most of the excess χ^2 comes from three measurements: the Johnson & Wilkinson balloon measurement, the South Pole measurement, and the fourth CN measurement. With this number of measurements, one or two 2σ results should be expected but here there are three.

Without the FIRAS measurements the weighted average is 2.729 ± 0.0038 which is 1.0σ from the final answer. Most

Table 2

Measurements and Uncertainties of the CMB Temperature

CMB Source	Temp (K)	Uncertainty (mK)	Reference
CN	2.700	40	Meyer & Jura (1985)
CN	2.740	50	Crane et al. (1986)
Balloon	2.783	25	Johnson & Wilkinson (1987)
CN	2.750	40	Kaiser & Wright (1990)
Rocket	2.736	17	Gush et al. (1990)
S Pole	2.640	39	Levin et al. (1992)
Balloon	2.712	20	Schuster et al. (1993)
CN	2.796	39	Crane et al. (1994)
CN	2.729	31	Roth et al. (1995)
Balloon	2.730	14	Staggs et al. (1996)
ARCADE1	2.694	32	Fixsen et al. (2004)
ARCADE1	2.721	10	Fixsen et al. (2004)
ARCADE2	2.731	5	Fixsen et al. (2009)
FIRAS	2.7249	1.0	Mather et al. (1999)
FIRAS	2.7255	0.85	Fixsen et al. (1996)
FIRAS	2.7260	1.3	This Work
Mean	2.72548	0.57	

of the weight (97%) of the final temperature estimate is from the FIRAS measurements. Each FIRAS measurement will be reviewed in turn.

The original concept of the FIRAS instrument was that the sky would be observed and the internal reference would be adjusted to minimize the signal. Then the external calibrator would be inserted and adjusted to match the signal from the sky. This method depends on knowing the calibration of the external calibrator germanium resistance thermometers. A 5 mK error in the original temperature determination of the external calibrator led directly to a 5 mK error in the temperature determination of the CMB. However, the calibration process corrects other effects of the error to first order (Fixsen et al. 1994). There were slight modifications to this plan (e.g., the internal reference was offset 10 mK for about half of the data), but basically the result is 2.7249 K (this has been rounded off to 2.725 in the literature), including the 5 mK correction for thermometer self-heating in the high current mode. The low current mode is noisy but there are $\sim 10^5$ measurements to compare the low current readings to the high current readings all at ~ 2.7 K. The final uncertainty depends on the calibration of the thermometers at NIST and the readout electronics. The uncertainty is estimated as 1 mK.

The second calibration of the FIRAS data is based on the color. The temperature can be determined from the color of the radiation if the frequency scale can be accurately determined. The frequency scale is derived from FIRAS observations of the interstellar CO and [C I] lines at 1300, 867, 650, and 609 μm (Fixsen et al. 1996). These were chosen because they are bright enough to determine the frequency and they are in the same part of the spectrum as the CMB. The temperature scale was determined independently from 7 different combinations of the four detectors and three scan modes. These determinations agreed within their uncertainties and the weighted uncertainty is 0.2 mK. There is a common uncertainty of 0.82 mK due to the uncertainty of the frequency scale, which dominates the total uncertainty. The result is $2.7255 \text{ K} \pm 0.85 \text{ mK}$. The thermometer errors are only weakly coupled to the color temperatures. Indeed, when the first color temperature was published, it disagreed with the thermometer by 4.5σ . It was only with the discovery of the high current self-heating offset that the two measurements came into alignment. The uncertainty of this method is driven by the

uncertainty in the measurement of the frequency of the CO and [C I] lines.

Now there is a third independent method of precisely calibrating the FIRAS instrument. The velocity method was presented before with the COBE Differential Microwave Radiometer (DMR) data (Fixsen et al. 1996). However, the DMR data did not have sufficient velocity precision to fully exploit this method; the *WMAP* data do. Because the differential measurements from the FIRAS instrument are taken only 50 minutes (half of an orbit) apart with the instrument in substantially the same state this method has the least potential for systematic errors. These spectra have far more supporting data than the calibration data. Each of the *WMAP* frequencies can be used to construct velocity map which in turn can be used to construct a spectrum. These spectra can then be fit to a dB/dT spectrum with the temperature as the single adjustable parameter.

5. SUMMARY AND CONCLUSIONS

The calibration methods for the FIRAS have been described and the accuracy estimated. All of the recent precision estimates of the CMB temperature agree within 2.5 times their uncertainties. These estimates were made with a variety of methods from different platforms and different frequencies. Combining all of the estimates results in a very modestly elevated χ^2 and an improved absolute temperature estimation of 2.72548 ± 0.00057 K.

I thank the *WMAP* team for providing the smoothed sky maps in velocity units. A special thanks to J. Weiland and G. Hinshaw.

REFERENCES

- Crane, P., et al. 1986, *ApJ*, 309, 882
 Crane, P., et al. 1994, *ApJ*, 346, 136
 Dickey, J. M., & Lockman, F. J. 1990, *ARA&A*, 28, 215
 Diehl, R., et al. 1995, *A&A*, 298, 445
 Fixsen, D. J., et al. 1994, *ApJ*, 420, 457
 Fixsen, D. J., et al. 1996, *ApJ*, 473, 576
 Fixsen, D. J., et al. 1999, *ApJ*, 526, 207
 Fixsen, D. J., et al. 2004, *ApJ*, 612, 86
 Fixsen, D. J., et al. 2009, *ApJ*, in press
 Gush, H. P., Halpern, M., & Wishnow, E. 1990, *Phys. Rev. Lett.*, 65, 537
 Hartmann, D., & Burton, B. W. 1997, in *Atlas of Galactic Neutral Hydrogen* (Cambridge, UK: Cambridge Univ. Press), 243
 Haslam, C. G. T., et al. 1981, *A&A*, 100, 209
 Hinshaw, G., et al. 2009, *ApJS*, 180, 225
 Johnson, D., & Wilkinson, D. 1987, *ApJ*, 313, L1
 Kaiser, M. E., & Wright, E. L. 1990, *ApJ*, 356, L1
 Kelsall, T., et al. 1998, *ApJ*, 508, 44
 Levin, S., et al. 1992, *ApJ*, 396, 3
 Mather, J. C., et al. 1999, *ApJ*, 512, 511
 Meyer, D. M., & Jura, M. 1985, *ApJ*, 297, 119
 Roth, K. C., et al. 1995, *ApJ*, 420, 457
 Schuster, J., et al. 1993, *ApJ*, 412, L47
 Staggs, S., et al. 1996, *ApJ*, 473, L1
 Standish, E. M., & Fienga, A. 2002, *A&A*, 384, 322